Supplementary Information for: "Tailoring van der Waals interactions in ultra-thin two dimensional metal-organic frameworks for photoconductive applications"

David Dell'Angelo,* Ioannis Karamanis, and Michael Badawi†

Université de Lorraine, CNRS, L2CM, F-57000 Metz, France

Mohammad Reza Saeb

Department of Pharmaceutical Chemistry,

Medical University of Gdańsk, J. Hallera 107, 80-416 Gdańsk, Poland

Lavinia Balan‡

CEMHTI-UPR 3079 CNRS, Site Haute Température,

1D avenue de la Recherche Scientifique, 45071 Orl éans, France

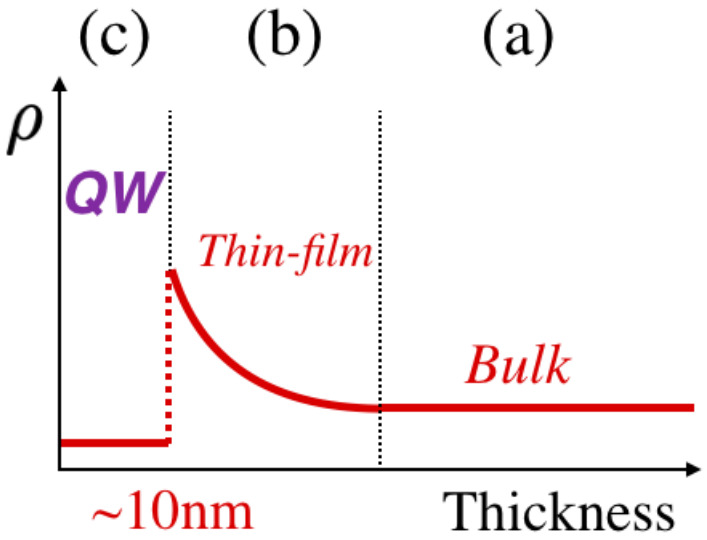

FIG. S1: Qualitative variation in 2D MOF resistivity (ρ) as a function of progressive vertical exfoliation. (a) ρ displays bulk characteristics; (b) the 2D confinement starts altering carriers flow and ρ starts increasing; (c) The De Broglie wavelength of the carrier becomes comparable to the quantum well (QW) thickness and ρ drops dramatically.[1]

TABLE S1: Set of parameter values used in the simulations of Figure 3 with $L_z = 2.97\ nm$. Parameters not included in the table are $J_{Coul} = 1100$, $E_{S1} = 2500\ cm^{-1}$ and absorption line width σ =650 cm^{-1}. λ values are: λ=1.1; λ_+=1; λ_-=0.8. All energy values are in $10^2\ cm^{-1}$.

$S_d = 3.5$ Å			
Fault slide (Å)	t_e^d	t_h^d	E_T^d
1.85†	6.12	5.20	3.7
2.05	4.92	-4.05	3.7
2.25	4.14	3.41	3.7
$S_d = 3.7$ Å			
Fault slide (Å)	t_e^d	t_h^d	E_T^d
1.85†	3.84	3.10	3.5
2.05	-2.93	2.4	3.5
2.25	2.13	1.65	3.5

† Exp. inter-layer sliding value from Ref. [4].

TABLE S2: Set of parameter values used in the simulations of Figure 4. Last two columns correspond to A1/A2 ratio at quasi-resonance (qR) and resonance (R) regimes, respectively. Parameters not included in the table are $J_{Coul} = 1100$ and $E_{T-S1} = 1400\ cm^{-1}$. The absorption line width is σ =650 cm^{-1}.

t_e (cm^{-1})	t_h (cm^{-1})	t_p ($10^5\ cm^{-1}$)	qR	R
880	900	7.92	1.105	1.381
830	850	7.05	1.052	1.292
780	800	6.24	1.012	1.242
680	700	4.76	0.924	1.073
580	600	3.48	0.853	0.975
480	500	2.40	0.785	0.890
376	380	1.43	0.697	0.853

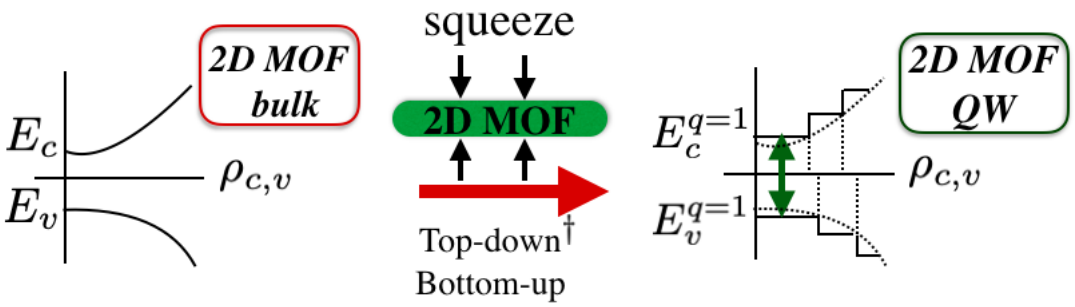

FIG. S2: In $Ni_3(HITP)_2$ bulk, the density profiles of the conduction and valence bands $D_{c,v}(E)$ depend on both energies $E_{c,v}$ and the effective masses $m^*_{c,v}$. By contrast, in the quantum well (QW) obtained along the $\pi-$stacking, $D_{c,v}(E) \propto m^*_{c,v}/L_z$ and the band gap E_g increases as $E_{g,QW} = E_c^{q=1} - E_v^{q=1}$ $(> E_{g,bulk} = E_c - E_v)$. For discussions on top-down and bottom-up techniques for generating ultra-thin 2D MOFs see Refs. [2,3].

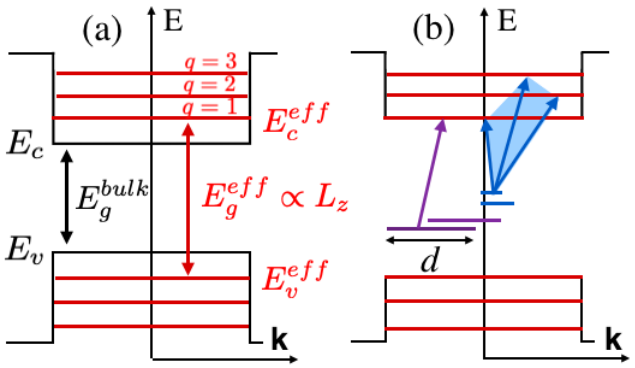

FIG. S3: $E-k$ diagram representation when the progressive exfoliation reaches the QW limit. (a) L_z determines both the number of states $(q = 1, 2, ..)$ in the QW and the effective bandgap E_g^{eff}. (b) In the presence of imperfections and trapped states, the probability of an upward transition depends on the uncertainty in the crystal momentum $(\propto \hbar/d)$.

TABLE S3: Set of parameter values used in the simulations of Figure 5. All values are in $10^4\ cm^{-1}$.

$E_{T-S1}(qR_1)$	$E_{T-S1}(qR_2)$	$E_{T-S1}(qR_3)$	$E_{T-S1}(R)$	$t_p(slide)$	$t_p(eclipsed)$	J_{Coul}
0.14	0.12	0.10	0	79.2	-79.2	1.1

TABLE S4: Hopping terms, units and values for calculating the charge transfer rates according to the Marcus Theory (Eq. 9), as displayed in Figure 8.

Hopping terms	Units	Values
T	K	Table S5
$t_{e/h}^{eclipsed}$	eV	Table S5†
t_{e}^{slide}	eV	Table S6
k_B	eV/K	8.61733E-05
λ	eV	Table S5
$\Delta G_e{}^{\text{II}}$	eV	-2.170‡
$\Delta G_h{}^{\mp}$	eV	-2.177‡
$\hbar$	eV $\times$ s	6.58212E-16
L_z	Å	59.4
μ_T	10^9/s	Table S5

† From Ref. [5], Figure 5.

$^{\text{II}}$ $[G_{anion} - G_{gs}] \cdot 27.2107 \frac{eV}{H}$

$^{\mp}$ $[G_{cation} - G_{gs}] \cdot 27.2107 \frac{eV}{H}$

‡ Sum of electronic and thermal free energies

TABLE S5: Calculated values for the eclipsed electron transfer rates as displayed in Figure 8. Units are given in Table S4.

N_{units} †	S^{II}	$\lvert t_e \rvert$	$\lvert t_h \rvert$	$\mu_{Te/h}{}^{\mathrm{a}}$	$\mu_{Te/h}{}^{\mathrm{b}}$	$\mu_{Te/h}{}^{\mathrm{c}}$
18	3.30	0.164	0.210	2.89/4.07	4.96/7.05	9.70/13.86
17	3.49	0.158	0.171	2.67/2.70	4.61/4.68	9.02/9.79
16	3.71	0.136	0.157	1.98/2.27	3.41/3.94	6.73/7.75
15	3.96	0.102	0.138	1.11/1.76	1.92/3.05	3.71/6.00

† Number of units in the π-stacking direction

II L_z/N_{units}

a $T_1 = 290,\ \lambda = 1.05$

b $T_2 = 296,\ \lambda = 1.06$

c $T_3 = 298,\ \lambda = 1.08$

TABLE S6: Calculated values for the slide electron transfer rates as displayed in Figure 8. Unit and parameter values are provided in Tables S4-S5. Superscripts a, b, and c are referring to the same T and λ values as in Table S3.

S^{II}	$\lvert t_e \rvert$	$\mu_T{}^{\mathrm{a}}$	$\mu_T{}^{\mathrm{b}}$	$\mu_T{}^{\mathrm{c}}$
3.30	0.149	2.38	4.10	8.01
3.49	0.139	2.07	3.57	6.97
3.71	0.125	1.68	1.88	5.64
3.96	0.082	0.72	1.24	2.43

I. DENSITY OF STATES FOR BULK AND ULTRA-THIN SHEET

Here we recall the theory of the density of states in E and k-space for both bulk and quantum well material.[6,7] Main expressions are summarized in Table 1 in the main text. In $Ni_3(HITP)_2$, atoms are arranged periodically. If we consider the (vertical) $\pi-$stacking dimension in the reciprocal space, this periodic arrangement leads to a periodic potential variation. In this periodic potential, Bloch's theorem states that solutions to the Schrödinger equation can be written as:

$$\Psi_k(r) = u_k(r)e^{ikr} \tag{1}$$

where k is the crystal momentum vector and $u_k(r)$ is a periodic function with the same periodicity as the crystal known as the periodic cell function. The energies of these states turn to be periodic in the wavenumber $k = \frac{2\pi}{\lambda_\omega}$, where λ_ω is the De Broglie wavelength of the carrier in the 2D framework. By applying an external electric field $\mathcal{E}$ to the system (Figure 4, main text), the net force on the carrier is due to

$$F = F_{ext} + F_{int} \tag{2}$$

where F_{int} corresponds to the crystal field. Provided the expression for the effective mass $m^* = \left(\frac{1}{\hbar^2}\frac{\partial^2 E}{\partial k^2}\right)^{-1}$, the crystal force field is already taken into account in the Bloch's wave-function and the carrier can move along the $\pi-$stacking direction as a plane wave. Thus, the crystal momentum $p = \hbar k$ responds only to F_{ext}, i.e. as a free particle

$$\frac{dp}{dt} = F_{ext} = -e\mathcal{E} \tag{3}$$

Since the medium confines the carrier propagation, $\Psi_k(r)$ must go to zero at the boundaries. The physical confinement also restricts the oscillation period of the wavefunction. According to the standing condition, the round trip phase of the wavefunction must be a multiple integer of 2π:

$$2kr = Q \cdot 2\pi \qquad Q = 1, 2, 3... \tag{4}$$

where the factor 2 on the LHS denotes the completion of a round trip phase kr. Since the carrier moves according to the three orthogonal components:

$$\mathbf{k} = \hat{i}k_x + \hat{j}k_y + \hat{k}k_z \tag{5}$$

with magnitude:

$$|\mathbf{k}| = \left(k_x^2 + k_y^2 + k_z^2\right)^{\frac{1}{2}}. \tag{6}$$

Each wavevector component must also satisfy:

$$2k_xL_x = m \cdot 2\pi \qquad m = 1, 2, 3...$$

$$2k_yL_y = p \cdot 2\pi \qquad p = 1, 2, 3...$$

$$2k_zL_z = q \cdot 2\pi \qquad q = 1, 2, 3...$$

This means that the three wavevector components are discretized as:

$$k_x^m = \left(\frac{\pi}{L_x}\right) m, \quad k_y^p = \left(\frac{\pi}{L_y}\right) p, \quad k_z^q = \left(\frac{\pi}{L_z}\right) q \tag{7}$$

Let us calculate now the density of states, i.e. the number of allowed states N_s between k and $k + dk$ per unit volume. In particular, *state* here means one allowed solution of the boundary value problem (Figure S4a). Because of the boundary conditions, one needs to consider only positive values of the k components, as negative values are already taken into account (Figure S4b). This means that in the spherical k-space, we need to consider only the positive octant (Figure S4c).

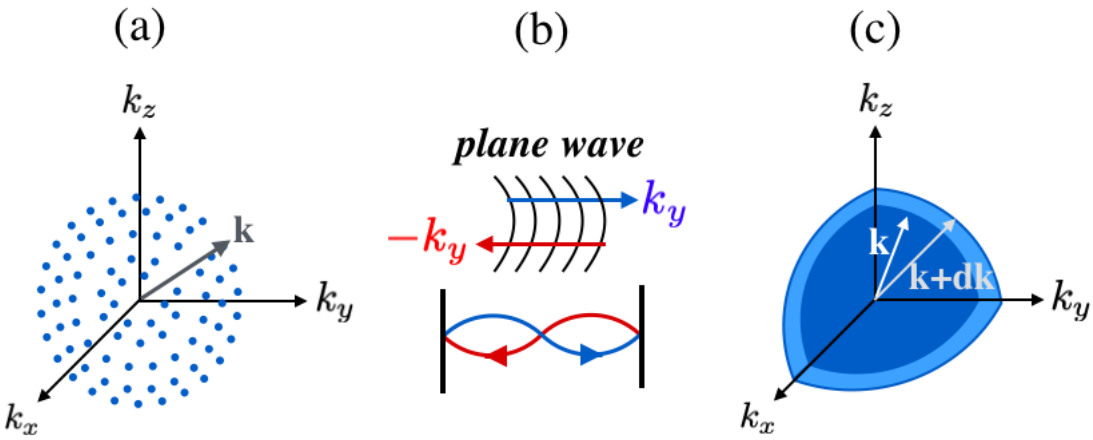

FIG. S4: (a) Representation of the allowed states in k-space. Each point represents one allowed state and k provides the direction along which the carrier is propagating. (b) Because of the standing wave boundary conditions, the negative direction of the k is automatically taken into account. (c) Only the positive k values (i.e., one octant) must be considered.

The volume occupied by one allowed state in k-space is:

$$V_s = \left(\frac{\pi}{L_x}\right)\left(\frac{\pi}{L_y}\right)\left(\frac{\pi}{L_z}\right) \tag{8}$$

thus, N_s is given by the volume between k and $k+dk$, i.e. the shell volume $= \frac{1}{8} \cdot 4\pi k^2 dk$, divided by V_s:

$$N_s = \frac{\frac{1}{8} \times 4\pi k^2 dk}{V_s} \times 2 \tag{9}$$

where the factor 2 on the RHS comes from the fact that there can be two electrons per state. In this definition, the density of states will be calculated as N_s per unit volume:

$$D(k)dk = \frac{N_s}{L_x L_y L_z} = \frac{k^2}{\pi^2} dk \tag{10}$$

To obtain the density in the E-space, since $D(E)dE = D(k)dk$,

$$D(E) = \frac{k^2}{\pi^2} \frac{dk}{dE} \tag{11}$$

In the conduction band, the energy of the electron is:

$$E = E_c + \frac{\hbar^2 k^2}{2m_c^*} \tag{12}$$

from which we can derive both k:

$$k = (E - E_c)^{\frac{1}{2}} \left(\frac{2m_c^*}{\hbar^2} \right)^{\frac{1}{2}} \tag{13}$$

and the first derivative of E with respect to k:

$$\frac{dE}{dk} = \frac{\hbar^2}{2m_c^*} 2k \tag{14}$$

By substitution of the previous two expressions in $D_c(E)$, one obtains the expression for the density of states:

$$\begin{aligned} D_c(E) = \frac{k^2}{\pi^2} \frac{dk}{dE} &= \left(\frac{k}{2\pi^2} \right) \left(\frac{2m_c^*}{\hbar^2} \right) \\ &= \frac{1}{2\pi^2} (E - E_c)^{\frac{1}{2}} \left(\frac{2m_c^*}{\hbar^2} \right)^{\frac{3}{2}} \end{aligned} \tag{15}$$

and for the valence band:

$$D_v(E) = \frac{1}{2\pi^2} (E_v - E)^{\frac{1}{2}} \left(\frac{2m_v^*}{\hbar^2} \right)^{\frac{3}{2}} \tag{16}$$

Let us move now to calculate the number of allowed states between k and $k+dk$ in the

quantum nanosheet. Whenever the L_z thickness becomes comparable to λ_ω of the carrier, z dimension is at nanoscale regime whereas k_x and k_y dimensions are still at the macroscale regime. The $in-$plane number of states $k_{in} = k_x \times k_y$ is still very large, yet the separation along z is increased and the allowed values for k_z becomes highly discretized with spacing equal to $\frac{\pi}{L_z}$ while the maximum number of allowed states are determined by $\frac{\pi}{S}$ (Figure S5). The reader is reminded that S corresponds to the interlayer distance and the lowest possible value of L_z is for the case when only 2 layers in the quantum nanosheet are assumed.

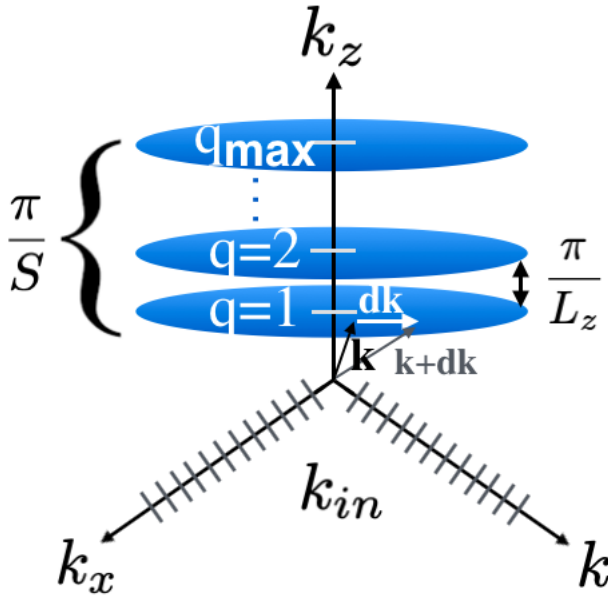

FIG. S5: High discretization along k_z as a result of reducing L_z dimension. Still, the number of $in-$plane allowed states (represented by the blue disc planes in the figure) remains very large.

k can be decomposed into an $in-$plane component *plus* the discretized component along z:

$$k = k_{in} + \hat{z}k_z \tag{17}$$

Correspondingly, the energy may be written as

$$E = E_c + \frac{\hbar^2 k_{in}^2}{2m_c^*} + E(q=1) \tag{18}$$

The number of points between k and $k + dk$ must correspond to the number of allowed states between k_{in} and $k_{in} + dk_{in}$:

$$D(k)dk = D(k_{in})dk_{in} \tag{19}$$

In the evaluation of the incremental vector dk_{in} (Figure S6), because of the boundary conditions one needs to consider only the positive quadrant in k-space:

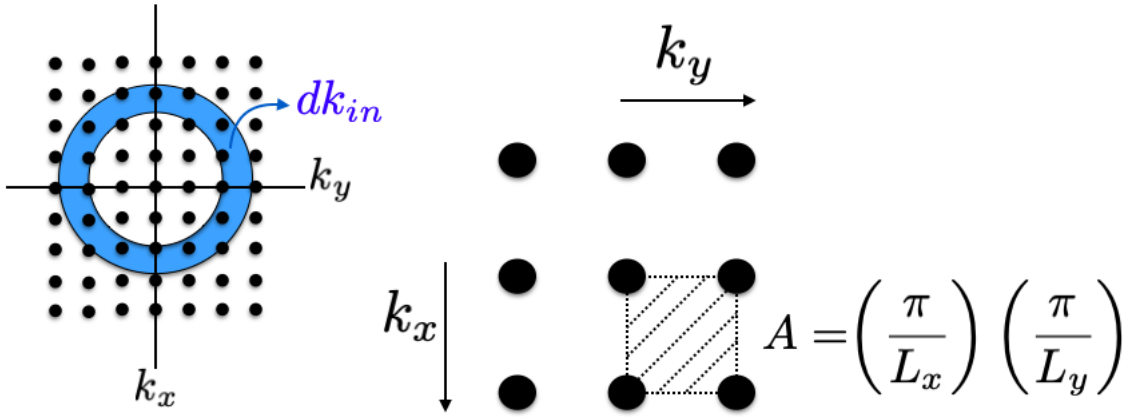

FIG. S6: Incremental vector dk_{in} and area of one point in k_{in} space.

$$n_{k_{in}} = \frac{\frac{1}{4} \times Area\{k_{in} + dk_{in}\}}{volume\ of\ one\ state} = \frac{\frac{1}{4} \times 2\pi k_{in} dk_{in}}{\left(\frac{\pi}{L_x}\right)\left(\frac{\pi}{L_y}\right)} \times 2 \tag{20}$$

Thus, the density of allowed states between k_{in} and $k_{in} + dk_{in}$ is provided by $n_{k_{in}}$ per unit volume:

$$D(k_{in})dk_{in} = \frac{\pi k_{in} dk_{in}}{\left(\frac{\pi}{L_x}\right)\left(\frac{\pi}{L_y}\right)} \times \frac{1}{L_x L_y L_z} = \frac{k_{in}}{\pi L_z} dk_{in} \tag{21}$$

The density in E space can be obtained from expression 18:

$$\frac{dE}{dk_{in}} = \frac{\hbar^2 k_{in}}{m_c^*} \tag{22}$$

Since $D(E)dE = D(k_{in})dk_{in}$,

$$D(E)dE = D(k_{in})\frac{dk_{in}}{dE} \tag{23}$$

By substituting the expression for $D(k_{in})$,

$$D_c(E) = \frac{D(k_{in})}{\left(\frac{dE}{dk_{in}}\right)} = \frac{\left(\frac{k_{in}}{\pi L_z}\right)}{\left(\frac{\hbar^2 k_{in}}{m_c^*}\right)} = \frac{m_c^*}{\hbar^2 \pi L_z} \tag{24}$$

Finally, the main implications in the momentum and energy space which stem from expression (24) can be summarized as follows :

(a) $D(E)$ does not depend on the energy (i.e., $D(E)$ is constant) but rather on the vertical

thickness of the 2D MOF;

(b) the $E-k$ diagram of the nano framework is characterized by sub-bands. To each sub-band corresponds a density of states D(E);

(c) because of the high discretization along k_z, the tip of the vector k (Figure S5,S7) may reach, depending on its energy, one of the disc planes characterized by increasing density;

(d) the densities in valence and conduction bands assume a step variation, as represented in Figure S2;

(e) the first allowed energy state along k_z in the nanolayer is at higher energy with respect to the bulk. The effective bandgap increases by an amount of the order of $\hbar/L_z$:

$$E_{g,eff} = E_g + \Delta E(q=1). \tag{25}$$

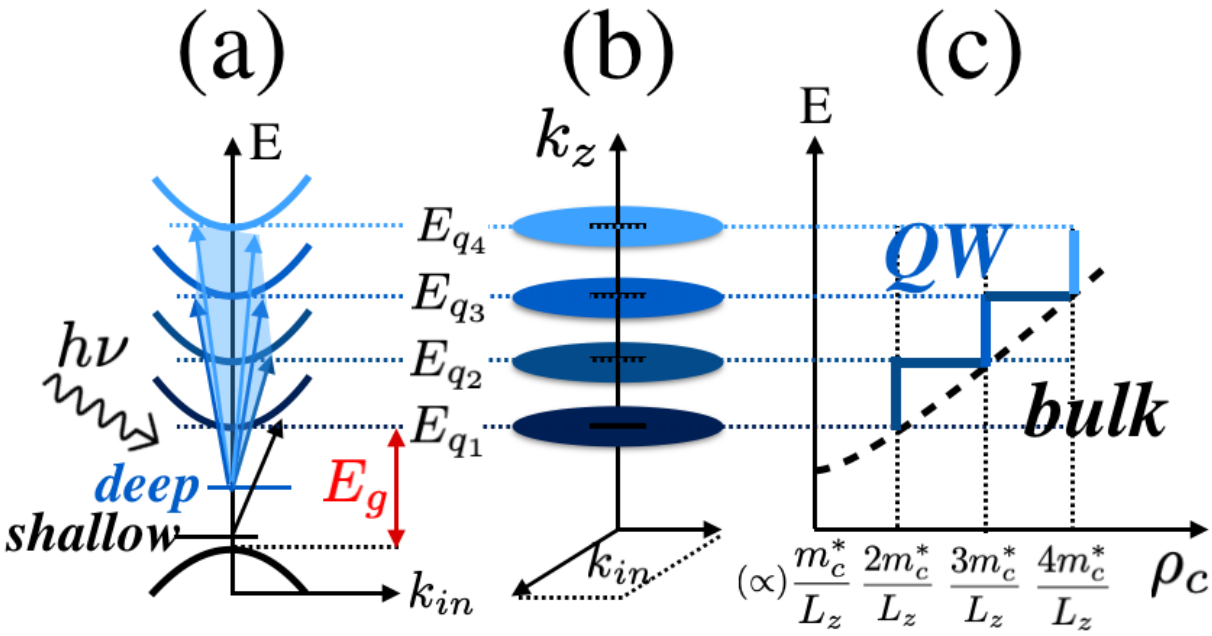

FIG. S7: Qualitative correlation between the conduction sub-bands (a), the discretization of the allowed states along k_z (b) and the step $\rho_c(E)$ profile as a result of the ultra-thin dimension L_z in $Ni_3(HITP)_2$ and discretization of the allowed states along k_z (c). In particular, (a) if the imperfection level is deep, the state is highly localized with a wavefunction that extends as far as the nearest neighbours. According to the indeterminancy principle, if the uncertainty ΔX in location is small, the one in k value Δk must be large. This means that transitions from imperfection level to a wide range of conduction sub-bands are possible and the tip of the k vector may reach a range of sub-bands (and discoid planes) (b)-(c). Conversely, for shallow imperfections this range is restricted essentially to one or two sub-bands (see also Figure S5).

* Electronic address: david.dell-angelo@univ-lorraine.fr

† Electronic address: michael.badawi@univ-lorraine.fr

‡ Electronic address: lavinia.balan@cnrs-orleans.fr

[1] V. Fatemi, S. Wu, Y. Cao, L. Bretheau, Q. D. Gibson, K. Watanabe, T. Taniguchi, R. J. Cava, and P. Jarillo-Herrero, Science **362**, 926 (2018).

[2] W. Zhao, J. Peng, W. Wang, S. Liu, Q. Zhao, and W. Huang, Coor. Chem. Rev. **377**, 44 (2018).

[3] W.-M. Liao, J.-H. Zhang, S.-Y. Yin, H. Lin, X. Zhang, J. Wang, H.-P. Wang, K. Wu, Z. Wang, Y.-N. Fan, et al., Nat. Commun. **9**, 2401 (2018).

[4] D. Sheberla, L. Sun, M. A. Blood-Forsythe, S. Er, C. R. Wade, C. K. Brozek, A. Aspuru-Guzik, and M. Dincă, J. Am. Chem. Soc. **136**, 8859 (2014).

[5] D. Dell'Angelo, M. R. Momeni, S. Pearson, and F. A. Shakib, J. Chem. Phys. **156**, 044109 (2022).

[6] S. V. Gaponenko, Electron states in an ideal nanocrystal (Cambridge University Press, 1998), p. 27–54.

[7] P. Y. Yu and M. Cardona, Fundamentals of semiconductors. Physics and materials properties. 4. ed. (Springer, Germany, 2010).